An interaction between α7 nicotinic receptors and a G-protein pathway complex regulates neurite growth in neural cells

Jacob C. Nordman and Nadine Kabbani*

Department of Molecular Neuroscience, Krasnow Institute for Advanced Study, George Mason University, Fairfax, Virginia 22030, USA

*Author for correspondence (nkabbani@gmu.edu)

Accepted 6 August 2012
Journal of Cell Science 125, 5502–5513
© 2012. Published by The Company of Biologists Ltd
doi: 10.1242/jcs.110379

Summary

The α7 acetylcholine nicotinic receptor (α7) is an important mediator of cholinergic transmission during brain development. Here we present an intracellular signaling mechanism for the α7 receptor. Proteomic analysis of immunoprecipitated α7 subunits reveals an interaction with a G protein pathway complex (GPC) comprising $G\alpha_{i/o}$, GAP-43 and G protein regulated inducer of neurite outgrowth 1 (Gprin1) in differentiating cells. Morphological studies indicate that α7 receptors regulate neurite length and complexity via a Gprin1-dependent mechanism that directs the expression of α7 to the cell surface. α7–GPC interactions were confirmed in embryonic cortical neurons and were found to modulate the growth of axons. Taken together, these findings reveal a novel intracellular pathway of signaling for α7 within neurons, and suggest a role for its interactions with the GPC in brain development.

Key words: Gprin, Axon growth, Proteomics, GAP-43, Cytoskeleton, Nicotine, Neurite, Bungarotoxin, Growth cone

Introduction

Neuronal development is marked by important phases in growth involving structural remodeling of the soma and an outgrowth of neurites culminating in the formation of functional axons and dendrites (Mortimer et al., 2008; Petros et al., 2008). Various neurotransmitter receptors are known to contribute to neuronal development (van Kesteren and Spencer, 2003; Mattson, 2008). Receptor mediated signal transduction appears crucial in regulating the assembly, disassembly, and reorganization of the cytoskeleton during growth (Stiess and Bradke, 2011). Signaling via the second messenger family of heterotrimeric GTP binding proteins (G proteins) is one mechanism for structural remodeling during neuronal development (Flavell and Greenberg, 2008). Inhibitory G proteins such as $G\alpha_{i/o}$ are enriched in developmental structures such as axonal growth cones during neurite navigation (Bromberg et al., 2008). In addition to being activated by membrane spanning G protein coupled receptors (GPCRs), $G\alpha_{i/o}$ can be activated by intracellular calcium (Strittmatter et al., 1991; Yang et al., 2009).

Calcium signaling is important during cellular development where it has been shown to play a role in the growth and navigation of newly formed neurites (Henley et al., 2004). Calcium-conducting ligand-gated ion channels, such as the nicotinic acetylcholine receptor (nAChR), are abundant during nervous system development and have been found to modulate the growth of neurons in the hippocampus and cortex (Zheng et al., 1994; Aramakis and Metherate, 1998). In differentiated neurons, nAChRs contribute to structural remodeling within presynaptic terminals and dendritic spines (Berg and Conroy, 2002). To date, 11 different nAChR subunits have been found in the mammalian brain (α2–α9 and β2–β4) (Albuquerque et al., 2009; Changeux, 2010). The α-bungarotoxin (Bgtx) sensitive α7 receptor is homopentameric and conducts mainly calcium upon activation (Dani and Bertrand, 2007). Previous studies indicate a role for α7 receptors in the growth of neurons and the formation of synapses (Coronas et al., 2000; Berg et al., 2006). Deactivation of α7 by ligands such as Bgtx as well as endogenous transmitters such as kynurenic acid (KYNA) has been found to impact neuronal growth (Stone and Darlington, 2002; Rüdiger and Bolz, 2008). To investigate the mechanisms by which α7 regulates neuronal development, we have determined the signaling properties of α7 receptors within differentiating neural cells. We present evidence on the existence of a G protein pathway complex (GPC), consisting of $G\alpha_{i/o}$, growth associated protein 43 (GAP-43), and G protein regulated inducer of neurite growth 1 (Gprin1), that directly associates with α7 in pheochromocytoma line 12 (PC12) cells and cortical neurons. α7–GPC interactions appear to modulate neurite and axonal development.

Results

α7 receptors mediate neurite growth

α7 receptors have been shown to affect neurite growth and synaptic development in neurons (Chan and Quik, 1993; Rüdiger and Bolz, 2008). To determine the role of α7 in neurite development we morphologically analyzed cells for growth using the Neuromantic software. In this study, cells with at least one process longer than the cell body were analyzed. We chronically treated PC12 cells with the α7 specific antagonist Bgtx, the nAChR agonist nicotine (Nic), the α7 specific agonist PNU282987 (PNU), or a combination of Bgtx and Nic or PNU during nerve growth factor (NGF) differentiation. Since all differentiation experiments were performed in the presence of

Journal of Cell Science

Journal of Cell Science

NGF, unless otherwise noted, the term differentiation is from here on synonymous with NGF-differentiation.

PNU, Nic, and Bgtx occupy a common binding site on the α7 receptor (Pankratov et al., 2002; Grabe et al., 2012b; Spitzer et al., 2012). As shown in Fig. 1A, chronic treatment with Bgtx resulted in a statistically significant increase in neurite surface area (SA) ($P<0.001$), while Nic and PNU treatments were found to significantly decrease neurite SA ($P<0.05$) compared to controls. A coapplication of Bgtx with Nic or Bgtx with PNU was found to result in a negligible morphological effect when compared to control cells ($P>0.05$) suggesting that the two drugs act via a common receptor. Group significance was found between control, Bgtx, Nic and PNU [$F(3,172)=4.00$, $P<0.001$]. Combination of PNU and Nic did not produce a greater effect on neurite SA than either drug alone (data not shown) consistent with the idea that PNU and Nic act via the same binding site (Pankratov et al., 2002). We next examined the effects of the endogenous transmitters acetylcholine (ACh) and KYNA, which are known to respectively activate or deactivate α7. As shown in Fig. 1A, chronic treatment with KYNA or ACh was found to significantly increase ($P<0.001$) or decrease ($P<0.05$) neurite SA, respectively [$F(2,184)=4.00$, $P<0.001$]. These effects of KYNA and ACh on neurite growth appeared comparable to the effects of Bgtx and Nic in the same cell line (Fig. 1A) and suggest that prolonged pharmacological perturbations of the α7 receptor mediates neurite growth within differentiating cells.

NGF induced differentiation of PC12 cells is known to promote RNA and protein synthesis, neurite growth, a decrease in cell division, electrical excitability, and render them more responsive to ACh (Csillik et al., 2004). We find that NGF promotes at least a twofold increase in neurite growth and branching complexity within PC12 cells (Fig. 1B). We assessed the role of nAChRs in PC12 cells in the absence of NGF. In comparison to NGF differentiated cells, PC12 cells grown in the absence of NGF displayed little or no neurite extension (Fig. 1B). Chronic treatment with ACh, Nic, or PNU was found to have little effect on neurite SA in the absence of NGF (data not shown). In contrast, chronic treatment with Bgtx was found to promote an increase in neurite growth even in the absence of NGF. As shown in Fig. 1B, Bgtx was found to increase neurite SA (compared to controls) in both differentiated and non-differentiated cells suggesting that the modulatory effects of Bgtx are not limited to NGF differentiation.

The cytoskeletal proteins actin and tubulin drive neurite extension and retraction during cellular growth (Zhou et al., 2002; Lowery and Van Vactor, 2009). We quantified the levels of α-tubulin and β-actin from lysates of cells chronically treated with Bgtx and Nic. As shown in Fig. 1C, α-tubulin expression was significantly increased in response to Bgtx ($P<0.05$) while significantly decreased after Nic treatment ($P<0.01$) in comparison to control cells. In these experiments, the levels of total β-actin in the cell did not appear to be significantly altered between Bgtx ($P=0.76$) and Nic ($P=0.55$) drug treatment conditions suggesting a role for these drugs on tubulin protein synthesis or stability.

Isolation of α7 interactomes

α7 has been implicated in the growth of neurites (Berg and Conroy, 2002) but the mechanism remains unknown. We tested antibodies (Abs) for their ability to detect the α7 subunit within PC12 cells. As shown in Fig. 2A two Abs directed again the α7 protein (mAb 306 and C-20) reacted to a ~57 kDa band within PC12 cell lysate (Fig. 2A, lane 1). In these experiments, Neuroblastoma 2a (N2a) cells were used as a negative control

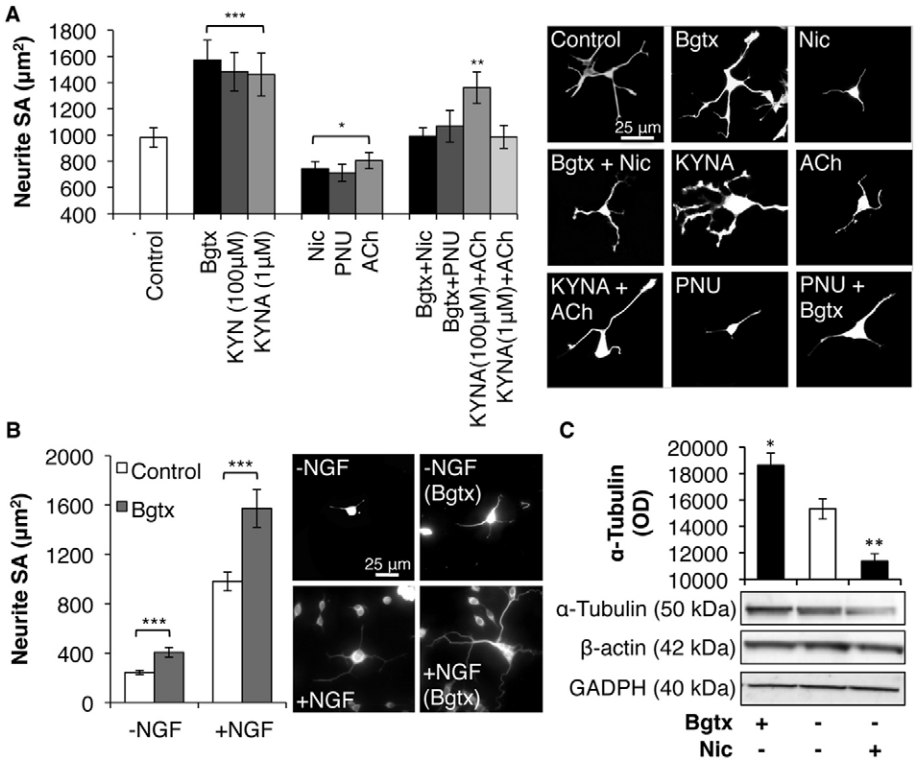

Fig. 1. α7 regulates neurite growth in PC12 cells. (**A**,**B**) Average neurite surface area (SA) and representative images of treated cells. Cells were stained with anti-α-Tubulin Abs. (A) Differentiated cells chronically treated with ACh and KYNA or Bgtx, Nic and PNU. (B) A comparison of neurite growth between NGF differentiated (+NGF) and non-differentiated (−NGF) cells. Bgtx was found to enhance neurite SA in +/−NGF cells. (**C**) Western blot detection of α-tubulin, β-actin, and GAPDH as a loading control within differentiating cells. Optical density (OD) analysis of α-tubulin levels in chronically treated cells.

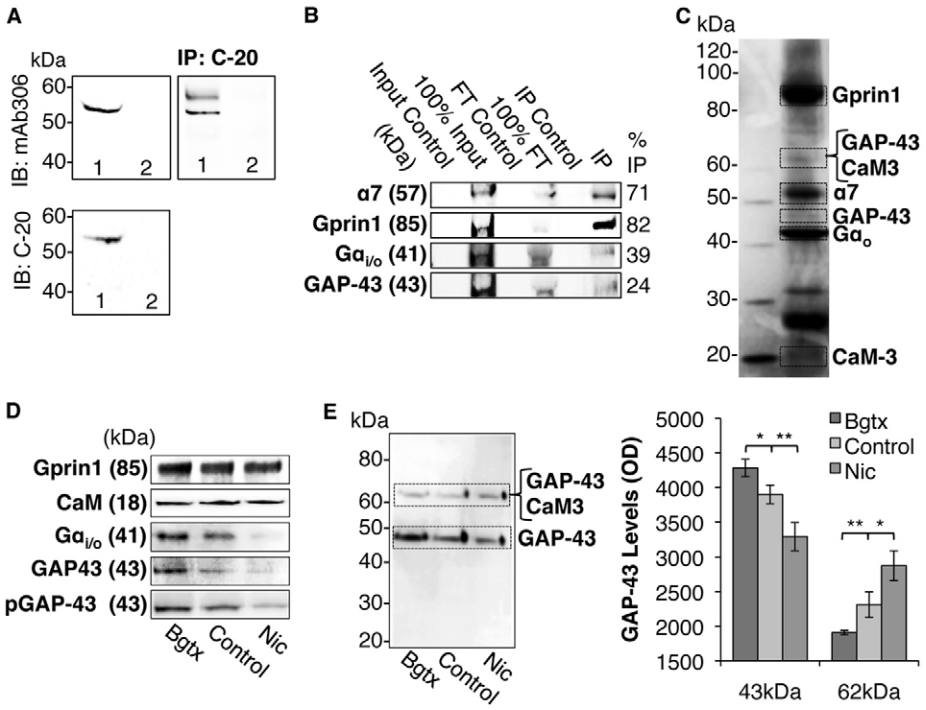

Fig. 2. Detection of α7/GPC interaction within differentiating PC12 cells. (**A**) IP and immunoblot (IB) detection of α7 from PC12 (lane 1) and N2a (lane 2) cells. Left, IB detection of α7 from total cell lysates. Right, IB detection of α7 within C-20 IP experiments. (**B**) IB detection of GPC proteins that coIP with the α7 subunit using C-20 (lanes are described in Materials and Methods). (**C**) A Coomassie stained gel showing the position of bands within the C-20 IP. The identity of proteins within the boxes was obtained using LC-ESI MS (supplementary material Table S2). (**D**) C-20 was used to coIP α7 receptor interacting proteins from PC12 cells treated with Bgtx/Control/Nic for 2 hr. IB detection of Gprin1, CaM, $G\alpha_{i/o}$, GAP-43, and phospho-GAP-43 within the IP. (**E**) IB detection of GAP-43 within crosslinked lysates of PC12 cells treated with Bgtx/Control/Nic for 2 hr. LC-ESI MS was used to verify the identity of the boxed 43 kDa and 61 kDa immunoreactive bands as GAP-43 and CaM3 bound GAP-43, respectively (supplementary material Table S3). Histogram: OD measurements of the two GAP-43 reactive bands in the blot.

since they do not express α7 (Fig. 2A, lane 2) (Danthi and Boyd, 2006). As shown in Fig. 2A, a polyclonal anti-α7 Ab (C-20) was able to successfully immunoprecipitate (IP) the α7 subunit from PC12 cells and in these IP experiments, two reactive bands were visualized on a western blot immunoprobed with mAb306 (Fig. 2A). Since α7 receptors can be glycosylated as well as palmitoylated (Hu et al., 2007), it is possible that these bands represent post-translational modifications to the α7.

Receptor-protein interactions mediate the trafficking and signaling of the receptor within the cell (Kabbani et al., 2007; Kabbani and Levenson, 2007; Yamatani et al., 2010). To determine interactions of α7, we utilized MS to define proteins that coIP with the α7 subunit in PC12 cells. In these experiments protein complexes that bound to the protein G matrix in the absence of the IP Ab were excluded from the results. Liquid Chromatography Electro Spray Ionization (LC-ESI) mass spectrometry (MS) analysis of IP complexes using mAb306 or C-20 reveals the presence of an α7 interaction complex. A list of α7 interacting proteins and information on their protein score (PS), molecular weight, and NCBI accession number is presented in supplementary material Table S1. A cohort of α7 interacting proteins are components of G protein pathways and are known to play a role in neurite development (supplementary material Table S1). We refer to this group as the GPC. Notably, $G\alpha_o$ and Gprin1 have been previously shown to interact with the β2 subunit of nAChRs in the adult brain (Kabbani et al., 2007) and have been found to direct growth cone and neurite development (Chen et al., 1999; Nakata and Kozasa, 2005; Masuho et al., 2008).

To validate α7–GPC interactions, C-20 was used in IP experiments from differentiating PC12 cells. Interacting proteins were visualized using western blot. As shown in Fig. 2B, a band immunoreactive for mAb306 was detected at 57 kDa, the expected molecular weight of the α7 subunit. Since previous studies have shown an interaction between $G\alpha_{i/o}$ and Gprin1 (Nakata and Kozasa, 2005) as well as $G\alpha_{i/o}$ and the guanine exchange factor (GEF) GAP-43 (Yang et al., 2009), we examined the presence of Gprin1, $G\alpha_{i/o}$ and GAP-43 within the same α7 complex. The blot shown in Fig. 2B was probed for Gprin1 and then reprobed using an anti-$G\alpha_{i/o}$ Ab and an anti-GAP-43 Ab. Immunoreactive bands corresponding to Gprin1, $G\alpha_{i/o}$, and GAP-43 were detected within the α7 complex. α7–GPC interaction was also found in non-differentiated PC12 cells at lower abundance (data not shown).

To confirm the presence of the α7–GPC interactomes C-20 was used to IP α7 from crosslinked cellular lysates of differentiated PC12 cells. As shown in Fig. 2C, a multi-protein complex was visualized using a Coomassie stain. Manually excised bands were analyzed using LC-ESI MS analysis. This confirmed the identity of Calmodulin 3 (CaM3, 18 kDa), $G\alpha_o$ (41 kDa), GAP-43 (43 kDa), Gprin1 (85 kDa), the α7 subunit (57 kDa), and GAP-43 bound to CaM3 (61 kDa) within a common complex.

α7 interactions regulate phosphorylation of GAP-43 and association with calmodulin

G proteins have been shown to regulate cytoskeletal dynamics and neurite growth in neurons (Rashid et al., 2001; Di Giovanni et al., 2005). In particular $G\alpha_{i/o}$ has been found in regions where cytoskeletal remodeling is high (Skene, 1989; Bromberg et al., 2008; Lowery and Van Vactor, 2009). We examined the effect of α7 on GPC interactions within PC12 cells. CoIP experiments using C-20 were performed on differentiated cells treated with Bgtx or Nic for 2 hours. As shown in Fig. 2D, western blot detection of IP α7 complexes reveals that treatment with Bgtx or Nic has no effect on Gprin1 and CaM levels within the complex. However, since the anti-CaM Ab used does not distinguish between various forms of CaM, changes in specific isoforms of CaM cannot be excluded. A reprobe of the membrane reveals

Journal of Cell Science

Journal of Cell Science

that Bgtx increases while Nic decreases the presence of $G\alpha_{i/o}$ and GAP-43 (Fig. 2D) within the α7 complex indicating that pharmacological activation of the receptor impacts its interaction with select GPC proteins.

The phosphorylation of GAP-43 by protein kinase C (PKC) (Esdar et al., 1999) and CaMKII (Denny, 2006; Leu et al., 2010) or dephosphorylation by calcineurin (PP2B) (Liu and Storm, 1989; Madsen et al., 1998) has been shown to regulate CaM association and neurite growth. In its unphosphorylated form, GAP-43 binds CaM leading to an inhibition in neurite growth (Skene, 1990; Slemmon et al., 1996). In contrast, phosphorylation of GAP-43 promotes CaM dissociation leading to an increase in neurite growth (Strittmatter et al., 1994b). An anti-phospho-GAP-43 Ab (selective for CaMKII phosphorylation site Serine 41) (Denny, 2006) was used to determine the effects of Bgtx and Nic on GAP-43. As shown in Fig. 2D, an increase in anti-phospho-GAP-43 immunoreactivity was observed within the α7 complex following Bgtx treatment. Similarly, Nic was found to decrease anti-phospho-GAP-43 immunoreactivity within the α7 complex. To determine if change in GAP-43 phosphorylation correlated with CaM binding, we utilized the bis(sulfosuccinimidyl) substrate (BS_3) to test the effects of Bgtx and Nic on GAP-43/CaM interaction. This method has been used in the detection of GAP-43 in the CaM bound/free states where the GAP-43 band runs at ~18 kDa (the approximate size of CaM) heavier on an SDS-PAGE gel when bound to CaM (Gamby et al., 1996). In these experiments, cell fractions were crosslinked following a 2-hour treatment with Bgtx, Nic, or a vehicle control. An anti-GAP-43 Ab was used to visualize two distinct bands within the sample and MS was used to confirm their identity as GAP-43 [bound to CaM3 (61 kDa) or alone (43 kDa)] (Fig. 2E). In control cells, the 43 kDa band presented a stronger signal than the 61 kDa band suggesting that CaM free GAP-43 is a main form of GAP-43 within PC12 cells. Densitometric analysis showed that the band at 43 kDa increased during Bgtx treatment and decreased during Nic treatment. In contrast, the band at 61 kDa increased during Nic treatment and decreased following Bgtx (Fig. 2E). In light of the differential associations between α7 and GAP-43 under these conditions, and the observed increase in phospho-GAP-43 reactivity with the α7 complex in the same cells (Fig. 2D), it is possible that Bgtx promotes interaction between α7 and non-CaM bound GAP-43 during growth.

α7 Receptors direct growth through $G\alpha_{i/o}$ and calmodulin

$G\alpha_{i/o}$ has been shown to regulate neurite growth (Strittmatter et al., 1994a; Swarzenski et al., 1996). To examine the role of $G\alpha_{i/o}$ in α7 signaling, we applied the $G\alpha_{i/o}$ inhibitor Pertussis toxin (Ptx) or the $G\alpha_o$ activator Mastoparan (MSP) during NGF differentiation (Fig. 3A). We tested the involvement of $G\alpha_{i/o}$ in Bgtx mediated neurite growth by exposing cells to both Ptx and Bgtx during the 4 days of NGF differentiation. As shown in Fig. 3B, coapplication of Ptx and Bgtx was found to significantly reduce neurite SA when compared to Bgtx treatment alone ($P<0.01$). When applied alone Ptx was found to decrease neurite SA to an average level below control cells (Fig. 3B). Since Nic was found to attenuate neurite growth during differentiation, we examined the ability of MSP to enhance neurite growth. A 4-day treatment with MSP was found to significantly increase neurite SA ($P<0.01$) (Fig. 3B) when compared to controls confirming the role of $G\alpha_{i/o}$ in neurite development. In the presence of Nic, MSP was found to only moderately promote neurite growth when compared to controls ($P=0.56$) (Fig. 3B) suggesting that MSP and Nic function antagonistically within the cell. Group significance was found between control, Ptx and MSP treatments [$F(2,135)=4.03$, $P<0.001$]. These studies underscore the role for $G\alpha_{i/o}$ in neurite development and suggest a functional interaction between $G\alpha_{i/o}$ and α7 in growth.

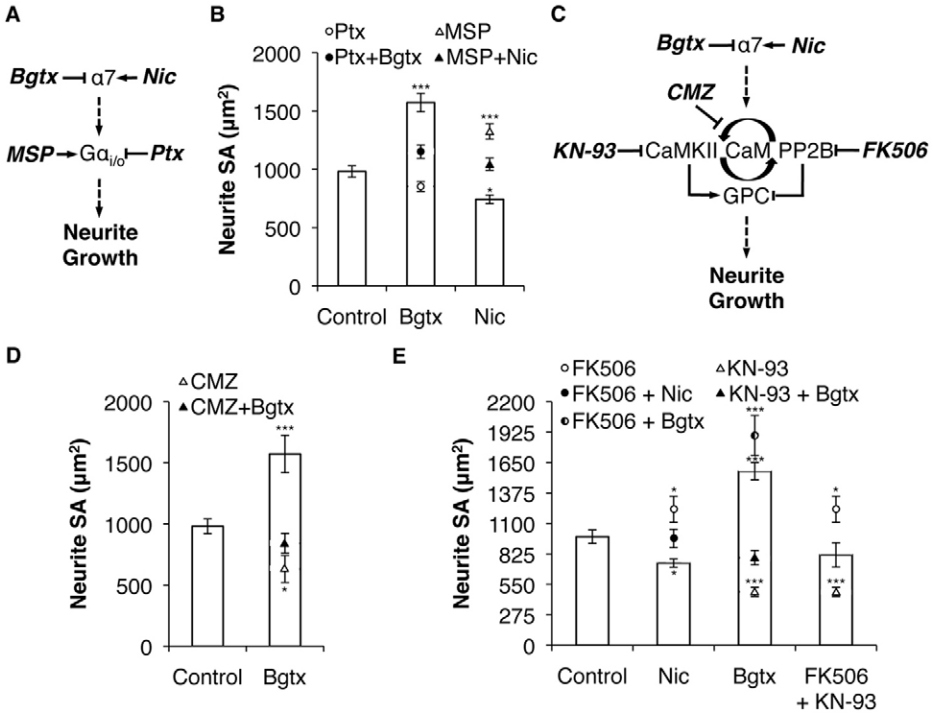

Fig. 3. Elucidating a GPC pathway mechanism in neurite growth. (**A**) A schematic diagram of $G\alpha_{i/o}$ function within the α7 pathway. Drugs and their targets are shown in bold italics. (**B**) Average neurite SA for cells chronically treated with Bgtx, Nic, Ptx, MSP, a combination of Ptx and Bgtx or MSP and Nic. (**C**) A schematic diagram of CaM, CaMKII, and PP2B within the α7 pathway. Drugs and their targets are shown in bold italics. (**D**) Average neurite SA for cells chronically treated with Bgtx, CMZ, or a combination of CMZ and Bgtx. (**E**) Average neurite SA for cells treated with Bgtx, Nic, FK506, KN-93, or a combination of FK506 and Nic, FK506 and Bgtx, KN-93 and Bgtx, or FK506 and KN-93.

Journal of Cell Science

The ubiquitous calcium sensor protein CaM (Liu and Berg, 1999; D'Alcantara et al., 2003) and a number of CaM regulated phosphoproteins including PP2B and CaMKII were identified as components of the α7 interaction network (supplementary material Table S1). We utilized drugs that block CaM, PP2B, and CaMKII to test the role of these proteins in α7 mediated neurite growth (Fig. 3C). As shown in Fig. 3D, we exposed cells to the CaM inhibitor calmidazolium (CMZ) during NGF differentiation. CMZ has also been shown to have some CaM independent effects including activation of phospholipase 2A and regulation of intracellular Ca^{2+} stores (Duffy et al., 2011). We find that CMZ produced a significant decrease in neurite SA when compared to controls ($P<0.01$), confirming that attenuation of CaM activity reduces neurite growth (Jian et al., 1994). To confirm the effects of CMZ on α7 signaling, we coapplied Bgtx and CMZ during differentiation. As shown in Fig. 3D, this combination was found to block the effects of Bgtx on neurite growth suggesting an important role for CaM in α7 signaling.

To investigate the role of PP2B and CaMKII, we probed the morphological effects of FK506 and KN-93, which respectively target these two proteins in cells (Liu and Berg, 1999; Jouvenceau and Dutar, 2006). As shown in Fig. 3E, application of FK506 was found to significantly increase neurite SA ($P<0.001$). This effect of FK506 was enhanced in the presence of Bgtx ($P<0.001$) and diminished in the presence of Nic ($P=0.87$), suggesting that Nic and PP2B operate synergistically to inhibit growth (Fig. 3E). Similarly, application of KN-93 was found to significantly diminish neurite SA when compared to control cells ($P<0.001$), suggesting that CaMKII activity is required for growth (Fig. 3E). Group significance was found between control, FK506, KN-93, and CMZ [$F(3,179)=3.36$, $P<0.001$]. When combined with Bgtx, KN-93 was found to block the effects of Bgtx on neurite SA (Fig. 3E) ($P>0.05$). These findings suggest that CaMKII operates downstream of α7 receptors in PC12 cells and is required for Bgtx mediated neurite growth. Finally, to confirm that PP2B and CaMKII operate within a common pathway (Fig. 3C), we coapplied KN-93 and FK506. This combination did not produce a significant change in neurite SA when compared to controls (Fig. 3E), suggesting that PP2B and CaMKII act antagonistically.

Gprin1 promotes α7 nAChR signaling and neurite growth

The $G\alpha_{i/o}$ interactor Gprin1 has been shown to regulate neurite growth in cells (Masuho et al., 2008; Ge et al., 2009). We examined interactions between α7 and Gprin1 in differentiating PC12 cells. Using a western blot we confirmed the ability of an anti-Gprin1 Ab to IP Gprin1 as well as α7 from cells (Fig. 4A). α7/Gprin1 interactions were further validated by heterologous protein expression studies in N2a cells, which do not express α7 (Danthi and Boyd, 2006). In these experiments we transiently transfected 1–10 μg of α7 cDNA (per 10 cm Petri dish of N2a cells) and tested for interaction with endogenous Gprin1 24 hrs later. As shown in Fig. 4B, α7 proteins were successfully detected in N2a cells after transfection. An IP of the α7 subunit from N2a cells reveal its association with endogenous Gprin1. A reverse IP of Gprin1 from N2a cells was also found to maintain an association with transfected α7 subunits (Fig. 4B).

We used a genetic knockdown strategy to test if Gprin1 mediates α7/GPC interaction. In these experiments, differentiating PC12 cells were transfected with plasmids encoding Gprin1 short interfering RNA (siRNA) ($Gprin1_{siRNA}$) (Ge et al., 2009). Western blot detection of Gprin1 within transfected cells reveals that $Gprin1_{siRNA}$ reduces Gprin1 levels

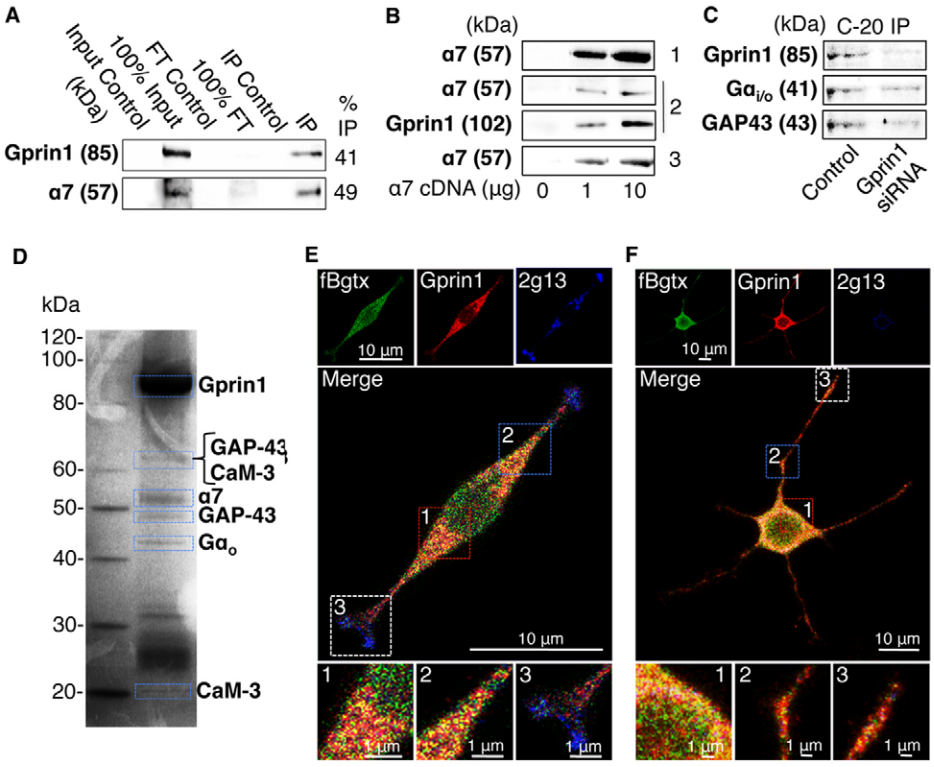

Fig. 4. α7/Gprin1 association within differentiating cells. (**A**) IB detection of α7 and Gprin1 within an IP of PC12 cells using an anti-Gprin1 Ab (lanes are described in Materials and Methods). (**B**) N2a cells were transiently transfected with 0, 1 and 10 μg of α7 cDNA. IB detection of α7 and Gprin1 from (1) total cell lysates, (2) C-20 IP, (3) Gprin1 IP of transfected cells. (**C**) IB detection of Gprin1, $G\alpha_{i/o}$, and GAP-43 within a C-20 IP. PC12 cells were transfected with $Gprin1_{siRNA}$ or an empty vector (Control). (**D**) A Coomassie stained gel showing the location of proteins that coIP with Gprin1. LC-ESI MS was used to identify proteins within boxed bands (supplementary material Table S4). (**E**,**F**) Confocal images of PC12 differentiated with NGF for 2 (E) and 4 (F) days. Cells were labeled with fBgtx (green), an anti-Gprin1 Ab (red), and an anti-2g13 Ab (blue). Merge panel shows colocalization of the three proteins within the cell. Insets: magnifications of soma (1), neurite (2), and a neurite terminal (3).

Journal of Cell Science

by 85% within cells (Fig. 6A). An IP of α7 was performed using C-20. As shown in Fig. 4C, in cells transfected with Gprin1 siRNA, α7 interactions with Gprin1, $G\alpha_{i/o}$ and GAP-43 appeared lower than control cells transfected with the empty vector. These findings suggest that Gprin1 expression plays a role in GPC interaction with α7. To test this, LC-ESI MS was used to analyze proteins that coIP with Gprin1 from PC12 cells. As shown in Fig. 4D, at least six discrete bands were visualized by a Coomassie stain of an SDS-PAGE gel loaded with proteins eluted from an anti-Gprin1 IP experiment. Based on MS identification, Gprin1, α7, CaM3, $G\alpha_{i/o}$ and GAP-43 were successfully detected within the Gprin1 IP experiment from PC12 cells, confirming Gprin1 interactions with α7 and GPC molecules.

We used fluorescein-conjugated Bgtx (fBgtx) and anti-Gprin1 Abs to colocalize endogenous α7 and Gprin1 within differentiating cells, respectively. As shown in Fig. 4E,F, α7 and Gprin1 proteins were found to colocalize within soma and growing neurites of differentiating PC12 cells. At 2 days of differentiation, Gprin1/α7 colocalization appeared prominent in the cytoplasm and near the cell surface and was seen uniformly distributed along the growing neurite and within the neurite terminal, which also stained positive for the growth cone marker 2G13 (Fig. 4E). At 4 days of differentiation, Gprin1/α7 colocalization was seen near the plasma membrane of the soma and in the growing neurites. However at this later stage of development, colocalization along the growing neurites appeared more punctuate and localized (Fig. 4F, boxes 2, 3).

Nicotine and Bgtx regulate α7 and Gprin1 levels at the plasma membrane

Nic has been found to differentially regulate the expression of nAChRs in cells (De Koninck and Cooper, 1995; Vallejo et al., 2005; Perry et al., 2007). We examined the effects of Bgtx and Nic on α7 expression and membrane localization within PC12 cells. Cells were chronically treated with Bgtx, Nic, or a combination of Bgtx and Nic during NGF differentiation. Cell surface biotinylation was then used to quantify protein expression at the plasma membrane. As shown in Fig. 5A, treatment with Bgtx was found to significantly increase ($P<0.001$) while treatment with Nic was found to significantly decrease α7 expression at the plasma membrane ($P<0.05$). Neither of the two drugs was found to have an effect on the expression of α4 subunits at the cell surface (Fig. 5A). A coapplication of Bgtx and Nic was found to have no effect on α7 expression at the cell surface relative to control cells ($P=0.42$). Because α7 interacts with Gprin1, we tested the effects of the drugs on Gprin1 levels at the plasma membrane. Western blot analysis of biotinylated proteins reveals that cell surface Gprin1 amounts are increased following Bgtx treatment ($P<0.001$) and decreased following Nic treatment ($P<0.05$), consistent with data on α7 levels at the membrane (Fig. 5A). These findings corroborate findings in Fig. 2D on constitutive interactions between Gprin1 and α7.

Confocal imaging was used to determine the effects of Bgtx and Nic/PNU on α7 and Gprin1 distribution. Distribution levels were determined using an assay where nine equidistant points

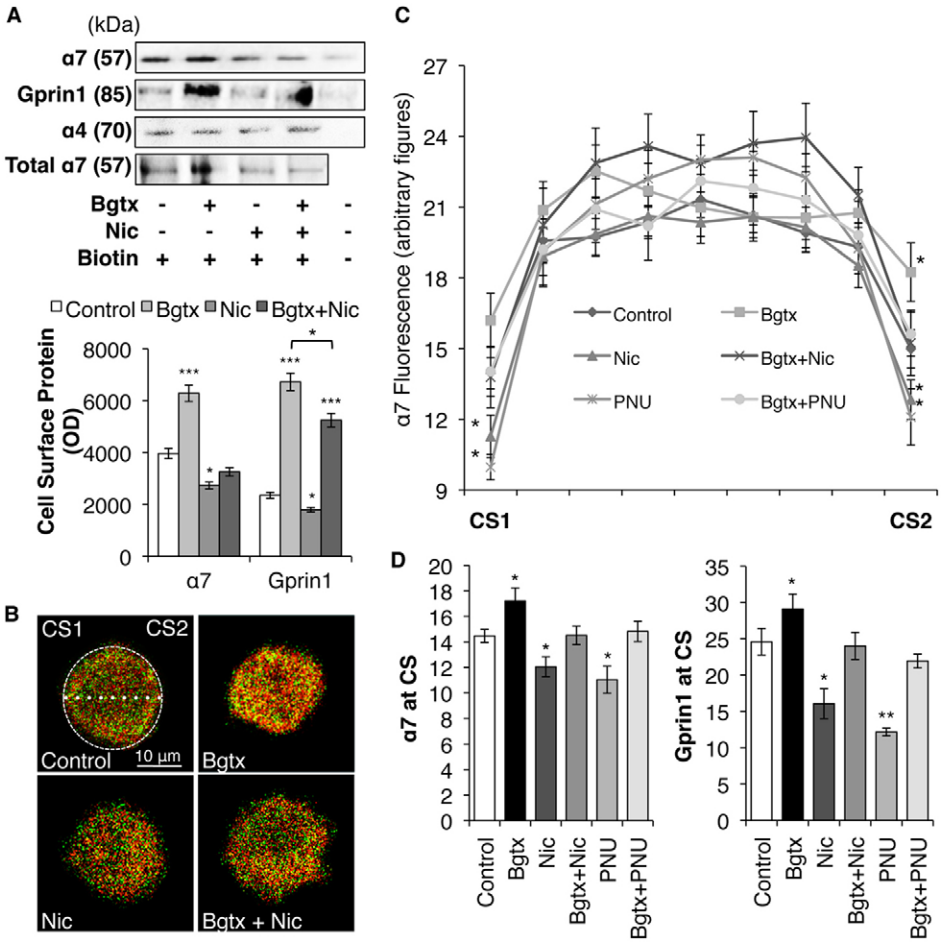

Fig. 5. Chronic drug treatment promotes changes in α7 and Gprin1 levels at the cell surface. (**A**) Cell surface biotinylation of differentiating cells chronically treated with Bgtx or Nic. IB detection and quantification of α7, Gprin1, and α4 at the cell surface following treatment. Non-biotinylated cells were used as a control in the assay. (**B–D**) A protein distribution assay was used to measure fluorescent signals for fBgtx and anti-Gprin1 at the cell surface (CS) and within the soma of non-differentiated PC12 cells. Cells were treated with Bgtx, Nic, PNU, or a combination of Bgtx and Nic or Bgtx and PNU for 24 hrs prior to fixation. (B) Images of representative cells labeled with fBgtx (green) and an anti-Gprin1 Ab (red). (C) Topographic distribution of the fBgtx signal within treated cells. (D) Average CS levels for α7 and Gprin1 following drug treatment.

were measured along the axis of a 2D image of a PC12 cell stained for fBgtx and anti-Gprin1 (de Lucas-Cerrillo et al., 2011) (Fig. 5B). Individual fluorescence signals for Gprin1 and fBgtx were significantly increased at the cell surface in cells chronically treated with Bgtx relative to controls. In contrast, fluorescence signals appeared weaker at the cell surface of cells chronically treated with Nic/PNU relative to controls (Fig. 5B–D; data not shown). Statistical significance was established between control, Bgtx, and Nic/PNU treatment groups: α7 [$F(3,312)=3.32$, $P<0.001$] and Gprin1 [$F(3,320)=3.32$, $P<0.001$]. In cells that received a combination of Bgtx and Nic/PNU, the signal for fBgtx and Gprin1 did not significantly differ from controls (Fig. 5B–D), confirming the opposing effect of these drugs on α7/Gprin1 levels at the plasma membrane.

Gprin1 expression regulates neurite growth

We utilized a genetic strategy to examine the role of Gprin1 on neurite growth in PC12 cells. In these experiments, cells were transiently transfected with plasmids encoding full length Gprin1 in pcDNA3.1 ($Gprin1_{pcDNA}$) or $Gprin1_{siRNA}$ (Ge et al., 2009) prior to differentiation. Transfected cells were then differentiated using NGF in the presence of Bgtx or Nic. Western blot detection of Gprin1 within transfected cells reveals that $Gprin1_{pcDNA}$ increases total Gprin1 expression by 98% whereas $Gprin1_{siRNA}$ decreases Gprin1 levels by 85% within cells (Fig. 6A). Total α7 levels were also increased in cells transfected with $Gprin1_{pcDNA}$ and modestly decreased in cells transfected with $Gprin1_{siRNA}$ (Fig. 6A). We did not observe a significant difference in Gprin1 protein expression between cells transfected with $Gprin1_{siRNA1}$ and $Gprin1_{siRNA3}$ (Fig. 6A). Cell surface biotinylation was used to determine the effects of $Gprin1_{pcDNA}$ and $Gprin1_{siRNA}$ on α7 and Gprin1 levels at the plasma membrane. As shown in Fig. 6B, $Gprin1_{pcDNA}$ was found to significantly increase while $Gprin1_{siRNA1/3}$ was found to significantly decrease α7 and Gprin1 levels at the cell surface. In these experiments, transfection of the empty vector did not alter the expression or the localization of α7 and Gprin1 within the cell (Fig. 6, control lanes).

Cellular imaging and morphometric analysis of cells expressing $Gprin1_{pcDNA}$ and $Gprin1_{siRNA3}$ reveals a dominant role for Gprin1 on α7 mediated neurite growth. As shown in Fig. 6C,D, transfection with $Gprin1_{pcDNA}$ was found to significantly increase neurite SA ($P<0.001$) while transfection with $Gprin1_{siRNA3}$ was found to significantly decrease neurite SA ($P<0.05$) in differentiated PC12 cells relative to controls. To examine the effects of Gprin1 on α7 mediated growth, we chronically treated cells with Bgtx, Nic, or PNU and compared their effect between cells transfected with $Gprin1_{pcDNA}$, $Gprin1_{siRNA3}$, or an empty vector control. As shown in Fig. 6C,D, $Gprin1_{siRNA3}$ was found to abolish the effect of Bgtx while $Gprin1_{pcDNA}$ was found to abolish the effect of Nic/PNU on neurite growth suggesting that Gprin1 expression at the cell surface is a main determinant of neurite growth and drug effect within these cells.

α7 Receptors interact with GPC and modulate axonal growth in cortical neurons

We tested the properties of Nic and Bgtx as well as ACh and KYNA on neurite development in primary cortical neurons. Using anti-MAP-2 and anti-Tau-1 Abs we analyzed the growth of dendrites and axons, respectively. Chronic treatment with nAChR

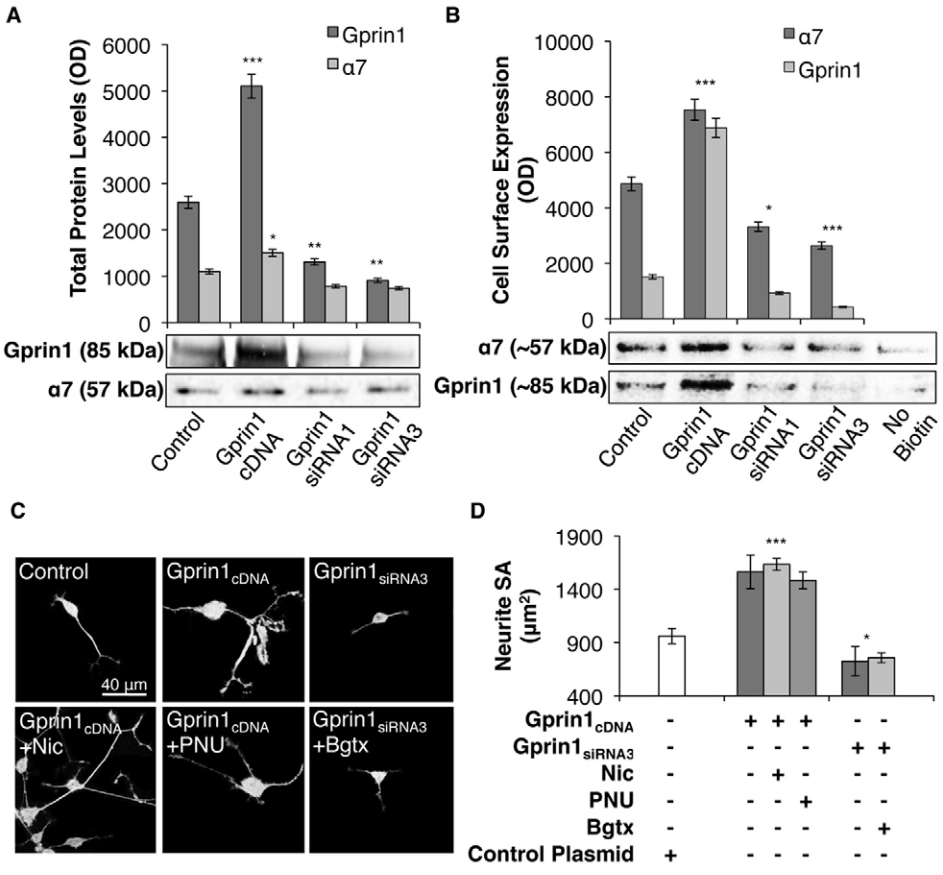

Fig. 6. Gprin1 regulates α7 levels at the cell surface and directs neurite growth in differentiating cells. PC12 were transiently transfected with plasmids for $Gprin1_{cDNA}$, $Gprin1_{siRNA}$, or an empty vector (Control). (**A**) Total protein levels of Gprin1 and α7 in transfected cells based on IB detection. (**B**) α7 and Gprin1 bands within biotinylated cells showing changes in protein levels at the cell surface. Non-biotinylated cells were used as a background control in the assay. (**C**,**D**) Transfected cells were chronically treated with Bgtx, Nic, or PNU. (C) Images of representative cells stained with anti-α-Tubulin Abs. (D) Histogram showing the effect of chronic drug treatment on neurite SA in $Gprin1_{pcDNA}$ or $Gprin1_{siRNA}$ transfected cells.

Journal of Cell Science

agonists (Nic/PNU/ACh) was found to significantly decrease axonal SA ($P<0.05$) while chronic treatment with α7 antagonists (Bgtx/KYNA) was found to significantly increase axonal growth and complexity of axons ($P<0.001$) (Fig. 7A,B). Group significance was found between control, Bgtx, Nic, PNU, KYNA, and ACh [$F(5,162)=2.77$, $P<0.001$]. Combining agonists and antagonists did not alter axonal growth relative to controls neurons (Bgtx and Nic, $P=0.40$; Bgtx and PNU, $P=0.23$; KYNA and ACh, $P=0.79$), and none of the drugs appeared to have a statistically significant effect on dendritic growth (data not shown).

Association between α7 and GPC proteins was confirmed in cortical neurons. As shown in Fig. 7C, a C-20 IP of the α7 subunit from cortical cells reveals the presence of Gprin1, $G\alpha_{i/o}$, and GAP-43 in association with α7 nAChRs. Interaction with Gprin1 was further validated using an anti-Gprin1 Ab that was able to coIP Gprin1 as well as α7 from the same neuronal lysates (Fig. 7C). Interaction between α7 and Gprin1 is likely to play an important role in axonal development as suggested by triple labeling fluorescence using fBgtx, anti-Gprin1, and phalloidin. As shown in Fig. 7D, colocalization of α7 and Gprin1 was seen in growing axons and within growth cones of cortical neurons suggesting a role for these proteins in axonal growth and guidance.

Discussion

To delineate mechanisms of α7 receptor function during development, we have used proteomics to define intracellular interactions of the α7 receptor within growing cells. PC12 cells have proven useful in studies of neuronal development since they endogenously express many neurotransmitter receptors (Connolly et al., 1979; Sarma et al., 2003). Once differentiated with NGF, PC12 cells extend elaborate neurites with the properties of growing axons (Drubin et al., 1985; Lee et al., 1998). We find that Bgtx and KYNA promote neurite growth in PC12 cells while enhancing axonal length and complexity in primary cortical neurons. ACh/Nic/PNU in contrast are found to attenuate neurite and axonal growth in PC12 cells and cortical neurons, respectively. It is noteworthy, that none of the drug treatment conditions appeared to significantly alter the percentage of cells with at least one process longer than the cell body (an inclusion criteria in the analysis) thus confirming that α7 receptor activity is associated with changes in neurite growth within differentiating cells. Our findings are consistent with earlier observations on the inhibitory effects of ACh on neurite development (Hieber et al., 1992; Lauder and Schambra, 1999) and suggest a role for α7 in structural and synaptic development (Corriveau et al., 1995; Romano et al., 1997). However, since nicotine and ACh activate other cholinergic receptors, the contribution of non-α7 receptors to neurite growth cannot be excluded. Likewise, the observed effects of KYNA on neurite and axonal growth (Figs 1, 7) complement data obtained from Bgtx treatment, and suggest that α7 inactivation plays a role in cellular function. Since KYNA is found to inactivate α7 and NMDA receptors (Pereira et al., 2002; Stone and Darlington,

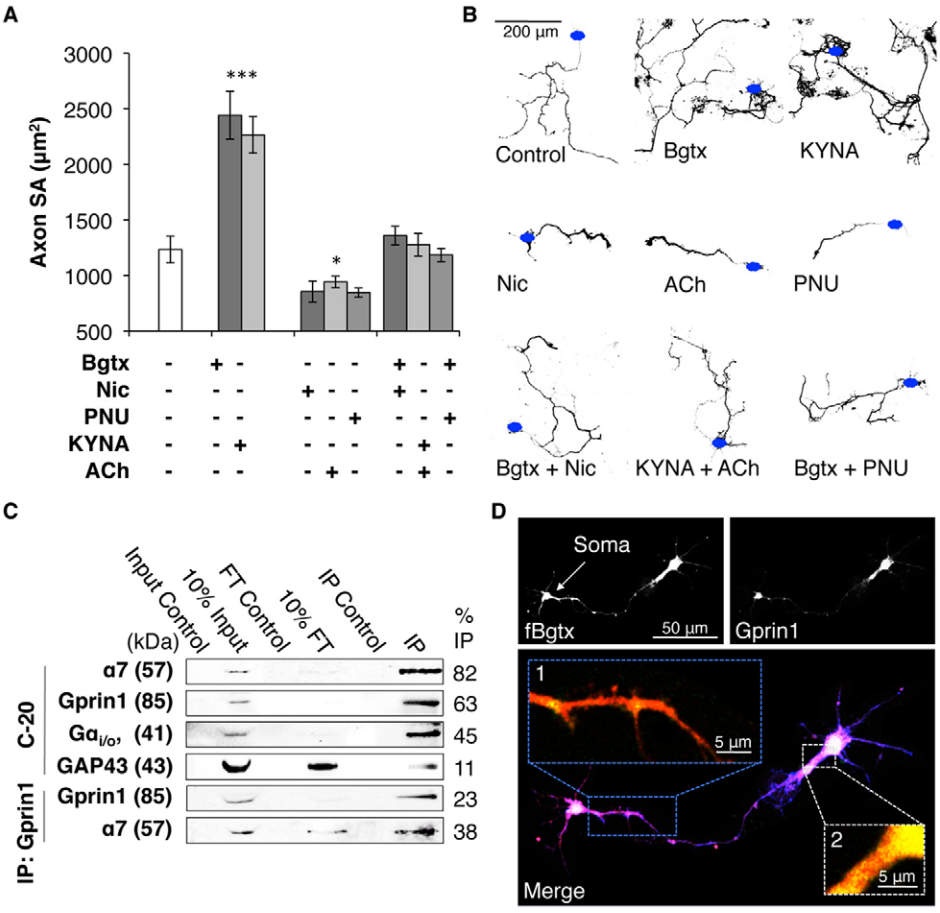

Fig. 7. Interactions of α7 and GPC in cortical neurons modulate axonal growth. Cortical neurons were cultured for 4 days in the presence of drugs. (**A**) An analysis of axonal SA in cortical neurons following chronic drug treatment. (**B**) Black and white contrast images of drug treated cells stained with anti-Tau-1 Abs in order to visualize growing axons. Soma indicated by a blue dot. (**C**) IB detection of α7 and GPC proteins within cortical neurons. Lysates from cortical neurons were IP using C-20 or anti-Gprin1 Abs. (**D**) A representative neuron colabeled with fBgtx and an anti-Gprin1 Ab. Single panels show the localization of α7 and Gprin1 within the soma and a growing axon. Merge panel shows colocalization of α7, Gprin1, and phalloidin within the cell. Insets: magnification of the axon (1) and the growth cone (2).

Journal of Cell Science

2002; Alkondon et al., 2007), it is possible KYNA contributes to synaptic development via its actions on these synaptic receptors (Lin et al., 2010).

Long-term cellular adaptations in neurotransmission include changes in receptor synthesis, turnover, and trafficking to and from the plasma membrane (Spitzer, 2012). To date little is known about the processes that direct nAChR synthesis and trafficking within growing cells. Studies have shown an effect of chronic Nic on the expression and composition of several nAChRs in various cell types (De Koninck and Cooper, 1995; Perry et al., 2007). Our data shows that chronic Nic decreases α7 while chronic Bgtx increases α7 expression at the cell surface in differentiating PC12 cells. Whether such drug-induced changes in receptor expression at the membrane correlate with changes in receptor activity such as desensitization or structural conformation is not clear. However, changes in α7 receptor levels at the membrane are found to shift downstream signaling via a Gprin1/GPC pathway producing important effects on neurite growth.

Gprin1 scaffolds α7/GPC signaling during growth

The $G\alpha_{i/o}$ interactor Gprin1 has been shown to localize to subcellular domains where cytoskeletal remodeling demands are high (Chen et al., 1999; Ge et al., 2009). Gprin1 association with the plasma membrane appears dependent on palmitoylation of cysteine residues within the G protein-binding site (Nakata and Kozasa, 2005). This along with its established role as a mediator of cytoskeletal regulating G proteins such as Cdc42 and Rac (Nakata and Kozasa, 2005; Masuho et al., 2008) suggests that Gprin1 is vital in neurite growth. We demonstrate an interaction between α7 and Gprin1 in growing cells and propose that this interaction links α7 to a GPC signaling apparatus as supported by the following key observations: (i) the ability of an anti-Gprin1 Ab to coIP α7 and GPC proteins from neurons and differentiating cells; (ii) colocalization of α7 and Gprin1 within growing neurites, axons, and growth cones; (iii) the ability of Gprin1 siRNA to decrease α7 expression at the cell surface or within the cell, reverse the effect of Bgtx on neurite growth, and attenuate interaction between α7 and GPC proteins. These findings confirm an important role for Gprin1 in scaffolding α7 receptors at the cell surface as shown for opioid receptors (Ge et al., 2009) and suggest that Gprin1 interactions facilitate the effects of α7 on growth. In addition, it is interesting to consider that Gprin1 interacts with β2 nAChRs (Kabbani et al., 2007) also present in PC12 cells, which may explain why changes in α7 expression at the cell surface are not entirely consistent with changes in Gprin1 levels at the cell surface following nicotine treatment (Fig. 5).

The existence of an α7–GPC network supports findings on associations between nAChRs and G protein signaling in cells (Kabbani et al., 2007; Paulo et al., 2009). Based on the current study we present a model for α7 signaling via the GPC during neurite development (Fig. 8). In this model we propose that ligand-induced changes in α7 levels (or conformation) at the cell surface direct GPC signaling towards inhibiting or promoting neurite growth. As shown in Fig. 8, drug-induced changes in receptor levels at the cell surface appear to accompany an overall effect on protein synthesis associated with growth. In one scenario, a decrease in α7 at the plasma membrane is found to promote inhibition of GPC function via the calcium sensitive phosphatase PP2B that is activated under conditions of low calcium levels (Stefan et al., 2008). As depicted in Pathway A, PP2B dephosphorylation of its target protein GAP-43 functions as an inhibitory switch for $G\alpha_{i/o}$ within the GPC pathway (Strittmatter et al., 1994b) and mediates interaction with CaM (Skene, 1990; Slemmon et al., 1996). This pathway is consistent with the finding that chronic Nic promotes enhanced GAP-43/CaM association and that a PP2B inhibitor (FK506) effectively blocks Nic induced neurite changes in PC12 cells.

In a second scenario, an increase in α7 levels at the plasma membrane appears to promote the GPC via CaMKII, which is activated under cellular conditions of higher calcium than PP2B (Wen et al., 2004). The contributions of CaMKII to this pathway, however, are supported by the ability of a CaMKII inhibitor to block Bgtx mediated neurite growth, because other calcium sensitive kinases such as PKC, also identified in our proteomic screen, can contribute to neurite growth in this scenario. As illustrated in Pathway B, CaMKII phosphorylation of its target protein GAP-43 functions as an activator of $G\alpha_{i/o}$ signaling within the cell. CaMKII phosphorylation of GAP-43 has also been shown to promote its dissociation from CaM (Denny, 2006; Leu et al., 2010), a finding consistent with our crosslinking experiments showing an effect of Bgtx on GAP-43/CaM dissociation within the cell (Fig. 2). This pathway is consistent with the effect of chronic Bgtx treatment on GAP-43 phosphorylation, or possibly the affinity of the α7 nAChR complex for phospho-GAP-43 interaction, as well as proteomic evidence showing that Bgtx mediates dissociation of GAP-43 and CaM within differentiating cells.

The proposed model explores the function of a novel GPC signaling pathway downstream of α7 nAChRs and alludes to the contributions of localized calcium signaling on the α7/GPC network. As suggested in Fig. 8, changes in calcium levels, from various sources including the α7 receptor may provide a trigger for the activity of high or low affinity calcium sensors such as PP2B or CaMKII, respectively. However calcium sources and

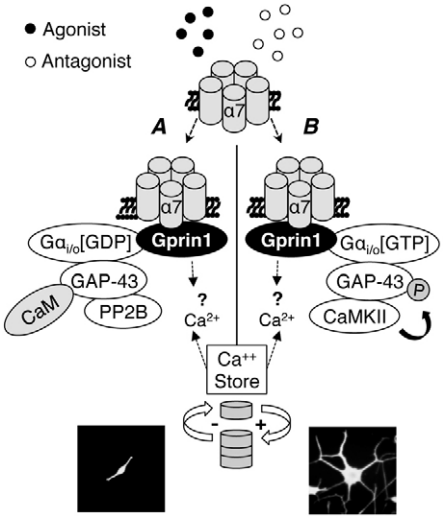

Fig. 8. A model for α7–GPC interactions in neurite growth. Exposure to agonist or antagonist is associated with changes in α7/Gprin1 levels at the plasma membrane. Pathway A: A decrease in α7/Gprin1 levels at the cell surface results in GPC inhibition via PP2B and a reduction in cytoskeletal mediated neurite growth. Pathway B: Increased α7/Gprin1 levels at the cell surface result in GPC activation via CaMKII and an increase in cytoskeletal mediated neurite growth. Both pathways are likely impacted by Ca^{2+} entry from external and internal sources.

Journal of Cell Science

targets within the pathway are not yet determined. Data presented in Fig. 3 for example, does not entirely demonstrate that PP2B and CaMKII function exclusively downstream of the α7 receptor in differentiating PC12 cells. Pharmacological suppression of these molecules appears slightly incomplete or additive in some experiments suggesting a function of two (or more) possible pathways in parallel within differentiating PC12 cells.

Materials and Methods

Cell culture

Pheochromocytoma line 12 (PC12) cells were grown on a rat collagen (50 μg/mL, Gibco) matrix in dMEM containing 10% horse serum, 5% fetal bovine serum (FBS), and 1% penicillin-streptomycin (Pen-strep) antibiotic. Cells were differentiated with 10 nM 2.5S nerve growth factor (NGF) for 4 days unless otherwise noted (Prince Laboratories). Primary neuronal cultures were obtained from embryonic day 18 Sprague-Dawley rats similar to what is described (Lin et al., 2001). Primary cultures were grown in Neurobasal media with B27 supplement and 1% Pen-strep. Human α7 in pcDNA1neo was provided by Dr Neil Millar (University College London) and has been previously described (Grabe et al., 2012a). Mammalian expression vectors encoding Gprin1 in pcDNA3.1 and Gprin1 siRNA in pRNAT H1.1 were provided by Dr Law (Univ. Minnesota) (Ge et al., 2009). These vectors express green fluorescent protein (GFP) under the same promoter (Ge et al., 2009). PC12 cells and Neuroblastoma 2a (N2a) cells were transfected using Lipofectamine 2000 as described by the manufacturer (Invitrogen). Cells were transfected with 1–10 μg/cm^2 α7 cDNA, 0.5 μg/cm^2 GFP-Gprin1 cDNA, or 20 pmol/cm^2 GFP-Gprin1 siRNA for 16 hours prior to media change. Transfected cells were identified using GFP fluorescence. An empty plasmid was used as a transfection control.

Drug treatment

Drug concentrations were determined based on published studies (Chan and Quik, 1993; Jian et al., 1994; Strittmatter et al., 1994a; Owen and Bird, 1995; Swarzenski et al., 1996; Hilmas et al., 2001; Kano et al., 2002; Hruska and Nishi, 2007; Lopes et al., 2007; Takemura et al., 2009): α-Bungarotoxin (Bgtx) (10 nM, Sigma), nicotine (Nic) (50 μM, Sigma), PNU282987 (PNU) (50 μM, Sigma), pertussis toxin (Ptx) (1 μM, Calbiochem), mastoparan (30 μM, Tocris), FK506 (25 nM, Tocris), KN-93 (1 μM, Tocris), calmidazolium (CMZ) (1 μM, Enzo), acetylcholine (ACh) (100 μM, Sigma) and KYNA (1:100 μM, Sigma). The duration of the *chronic* drug treatment described in this study is 4 days unless otherwise noted. All experiments were performed in triplicate and the data presented represents the average for each condition. At the end of each experiment cell viability was determined using Trypan Blue (EMD).

Immunocytochemistry

Cells were fixed using a 4% paraformaldehyde solution (250 mM sucrose, 25 mM HEPES HCO_3 free, 2.5 mM KCl; pH 7.2). Cells were permeabilized at room temperature using 0.1% Triton X-100 then immunostained overnight at 4℃ using one or several of the following primary antibodies (Abs): anti-α-Tubulin polyclonal (Sigma); anti-Gprin1 polyclonal (Abcam), anti-2g13 monoclonal (Serotec), anti-Tau-1 monoclonal (Millipore), anti-MAP-2 polyclonal (Abcam). Secondary Abs: carbocyanine (Cy) 2/3; Dylight 488; Dylight 560; and AlexaFluor 647 were purchased from Jackson-ImmunoResearch. α7 receptors were also visualized using a fluorescein-conjugated Bgtx (fBgtx) (Molecular Probes). Rhodamine Phalloidin was purchased from Cytoskeleton. All immunostainings were visualized using a Nikon Eclipse 80i confocal microscope fitted with a Nikon C1 CCD camera and images captured using AxioVision and EZ-C1 software.

Morphological and statistical analysis

Morphological reconstruction was performed using Neuromantic software (Myatt and Nasuto, 2008). Surface area (SA) was measured from cellular compartments (soma and neurites) to assess size and complexity under various conditions. 20–30 cells were reconstructed per condition and group averages were derived from three separate experiments. An image assessment of cells using differential interference contrast (DIC) microscopy confirmed an overlap of the tubulin immunosignal and the cellular contour. Statistical analysis was conducted on raw data of image tracing using Neuromantic. Statistical values have been obtained using a Student's *t* test or one-way ANOVA. Asterisks indicate statistical significance in a paired Student's *t* test, two tailed *P* value, * <0.05; ** <0.01; *** <0.001. Error bars indicate standard error of the mean (SEM).

Protein isolation and detection

Cell lysates were obtained from proteins solubilized in a non-denaturing lysis buffer (1% Triton X-100, 137 mM NaCl, 2 mM EDTA, and 20 mM Tris-HCl pH 8) with protease inhibitor cocktail (Complete) at 4℃ for 1 hour. Membrane fractions and immunoprecipitation of receptor complexes were conducted similarly to earlier described experiments (Kabbani et al., 2007). Immunoprecipitated (IP) complexes were obtained using an anti-α7 subunit monoclonal Ab (mAb306) (Lindstrom et al., 1990), an anti-α7 polyclonal Ab (C-20) [Santa Cruz Biotechnology (SC)], or an anti-Gprin1 rabbit polyclonal Ab (Abcam). Lysates incubated with the bead matrix, without an Ab, were used as IP controls. Membranes were blocked with 5% nonfat milk/BSA (for bis(sulfosuccinimidyl) substrate (BS_3, Pierce) crosslinking or biotinylation experiments) then probed with primary Abs overnight at 4℃. Gprin1 (Abcam); $G\alpha_{i/o}$ (SC); GAP-43 (Abcam); pGAP-43 (Abcam); α7 (SC); calmodulin (CaM, Millipore); α-Tubulin (Sigma); Actin (Sigma). Species-specific peroxidase conjugated secondary Abs were purchased from (Jackson-ImmunoResearch). Signals were detected using a SuperSignal West Pico Chemiluminescent Substrate (Thermo Scientific). SeeBlue and MagicMark (Invitrogen) were used as molecular weight standards. Blots were imaged using a Gel Doc Imaging system (Bio-Rad). Band density analysis in western blots was measured using NIH ImageJ. Fig. 2B, Fig. 4A, Fig. 7C: Input Control, no lysate; 100% Input, total lysate as used in the IP; FT Control, flow-through supernatant of Ab/bead conjugation; 100% FT; flow-through supernatant of IP; IP Control, no Ab; % IP=IP/Input×100. Western blot values are based on averages from three separate experiments.

Protein crosslinking and cell surface biotinylation

For substrate bound analysis of protein complexes, the irreversible crosslinker BS_3 (Pierce) was incubated with cell lysates at a concentration of 2.5 mM BS_3 for 30 min at room temp. The reaction was quenched using 50 mM Tris-HCl pH 7.5 then loaded onto Ab conjugated Protein G Dynabeads for IP of the crosslinked samples. The quantification of proteins at the cell surface was conducted using a cell surface biotinylation labeling protocol (Hannan et al., 2008). In these experiments 300 μg/mL EZ-Link Sulfo-NHS-LC-Biotin (Pierce) was used to label cell surface proteins in live cells for 30 min at 4℃. The biotin reaction was quenched using Tris-Buffered Saline (TBS) and membrane fractions were isolated for pull-down with a Neutravidin agarose bead matrix (Pierce) over a 30 μm pore size Snap Cap spin column (Pierce). Cell surface proteins were analyzed using western blot. Experiments were performed in triplicate.

Mass spectrometry

Protein analysis was conducted using Liquid Chromatography Electrospray Ionization (LC-ESI) mass spectrometry (MS). Protein complexes were prepared as described (Kaiser et al., 2008) and mass spectrometry was carried out using a published protocol (Gutiérrez et al., 2007). Tandem mass spectra collected by Xcalibur (version 2.0.2) were searched against the NCBI rat protein database using SEQUEST (Bioworks software from ThermoFisher, version 3.3.1). The SEQUEST search results were filtered using the following criteria: minimum X correlation (XC) of 1.9, 2.2, and 3.5 for 1+, 2+, and 3+ ions, respectively, and $\Delta Cn > 0.1$. The Protein Score (PS) represents the XC where scores <0.1 were excluded from the analysis and does not reflect the quantity of a protein in the sample.

Acknowledgements

We thank Sarah Clark and Dylan van Kampen for assistance with the study, and the Center for Applied Proteomics and Molecular Medicine at George Mason University for the generous use of instrumentation.

Funding

This study was supported by a Jeffress Memorial Research Grant Award [grant number J-953 to N.K.].

Supplementary material available online at
http://jcs.biologists.org/lookup/suppl/doi:10.1242/jcs.110379/-/DC1

References

Albuquerque, E. X., Pereira, E. F., Alkondon, M. and Rogers, S. W. (2009). Mammalian nicotinic acetylcholine receptors: from structure to function. *Physiol. Rev.* **89**, 73-120.

Alkondon, M., Pereira, E. F., Potter, M. C., Kauffman, F. C., Schwarcz, R. and Albuquerque, E. X. (2007). Strain-specific nicotinic modulation of glutamatergic transmission in the CA1 field of the rat hippocampus: August Copenhagen Irish versus Sprague-Dawley. *J. Neurophysiol.* **97**, 1163-1170.

Aramakis, V. B. and Metherate, R. (1998). Nicotine selectively enhances NMDA receptor-mediated synaptic transmission during postnatal development in sensory neocortex. *J. Neurosci.* **18**, 8485-8495.

Berg, D. K. and Conroy, W. G. (2002). Nicotinic α7 receptors: synaptic options and downstream signaling in neurons. *J. Neurobiol.* **53**, 512-523.

Berg, D. K., Conroy, W. G., Liu, Z. and Zago, W. M. (2006). Nicotinic signal transduction machinery. *J. Mol. Neurosci.* **30**, 149-152.

Bromberg, K. D., Iyengar, R. and He, J. C. (2008). Regulation of neurite outgrowth by $G_{i/o}$ signaling pathways. *Front. Biosci.* **13**, 4544-4557.

Chan, J. and Quik, M. (1993). A role for the nicotinic α-bungarotoxin receptor in neurite outgrowth in PC12 cells. *Neuroscience* **56**, 441-451.

Changeux, J. P. (2010). Nicotine addiction and nicotinic receptors: lessons from genetically modified mice. *Nat. Rev. Neurosci.* **11**, 389-401.
Chen, L. T., Gilman, A. G. and Kozasa, T. (1999). A candidate target for G protein action in brain. *J. Biol. Chem.* **274**, 26931-26938.
Connolly, J. L., Greene, L. A., Viscarello, R. R. and Riley, W. D. (1979). Rapid, sequential changes in surface morphology of PC12 pheochromocytoma cells in response to nerve growth factor. *J. Cell Biol.* **82**, 820-827.
Coronas, V., Durand, M., Chabot, J. G., Jourdan, F. and Quirion, R. (2000). Acetylcholine induces neuritic outgrowth in rat primary olfactory bulb cultures. *Neuroscience* **98**, 213-219.
Corriveau, R. A., Romano, S. J., Conroy, W. G., Oliva, L. and Berg, D. K. (1995). Expression of neuronal acetylcholine receptor genes in vertebrate skeletal muscle during development. *J. Neurosci.* **15**, 1372-1383.
Csillik, B., Mihaly, A. and Knyihar-Csillik, E. (2004). Cytochemical correlates of the sleep-wake interface: concerted expression of brain-derived nitric oxide synthase (bNOS) and the nicotinic acetylcholine receptor (nAChR) in a columnoid organization of the primate prefrontal cortex. *Ann. Anat.* **186**, 217-221.
D'Alcantara, P., Schiffrann, S. N. and Swillens, S. (2003). Bidirectional synaptic plasticity as a consequence of interdependent calcium controlled phosphorylation and dephosphorylation pathways. *Eur. J. Neurosci.* **17**, 2521-2528.
Dani, J. A. and Bertrand, D. (2007). Nicotinic acetylcholine receptors and nicotinic cholinergic mechanisms of the central nervous system. *Annu. Rev. Pharmacol. Toxicol.* **47**, 699-729.
Danthi, S. and Boyd, R. T. (2006). Cell specificity of a rat neuronal nicotinic acetylcholine receptor α7 subunit gene promoter. *Neurosci. Lett.* **400**, 63-68.
De Koninck, P. and Cooper, E. (1995). Differential regulation of neuronal nicotinic ACh receptor subunit genes in cultured neonatal rat sympathetic neurons: specific induction of α_7 by membrane depolarization through a Ca^{2+}/calmodulin-dependent kinase pathway. *J. Neurosci.* **15**, 7966-7978.
de Lucas-Cerrillo, A. M., Maldifassi, M. C., Arnalich, F., Renart, J., Atienza, G., Serantes, R., Cruces, J., Sánchez-Pacheco, A., Andrés-Mateos, E. and Montiel, C. (2011). Function of partially duplicated human α7 nicotinic receptor subunit *CHRFAM7A* gene: potential implications for the cholinergic anti-inflammatory response. *J. Biol. Chem.* **286**, 594-606.
Denny, J. B. (2006). Molecular mechanisms, biological actions, and neuropharmacology of the growth-associated protein GAP-43. *Curr. Neuropharmacol.* **4**, 293-304.
Di Giovanni, S., De Biase, A., Yakovlev, A., Finn, T., Beers, J., Hoffman, E. P. and Faden, A. I. (2005). *In vivo* and *in vitro* characterization of novel neuronal plasticity factors identified following spinal cord injury. *J. Biol. Chem.* **280**, 2084-2091.
Drubin, D. G., Feinstein, S. C., Shooter, E. M. and Kirschner, M. W. (1985). Nerve growth factor-induced neurite outgrowth in PC12 cells involves the coordinate induction of microtubule assembly and assembly-promoting factors. *J. Cell Biol.* **101**, 1799-1807.
Duffy, A. M., Fitzgerald, M. L., Chan, J., Robinson, D. C., Milner, T. A., Mackie, K. and Pickel, V. M. (2011). Acetylcholine α7 nicotinic and dopamine D2 receptors are targeted to many of the same postsynaptic dendrites and astrocytes in the rodent prefrontal cortex. *Synapse* **65**, 1350-1367.
Esdar, C., Oehrlein, S. A., Reinhardt, S., Maelicke, A. and Herget, T. (1999). The protein kinase C (PKC) substrate GAP-43 is already expressed in neural precursor cells, colocalizes with PKC*η* and binds calmodulin. *Eur. J. Neurosci.* **11**, 503-516.
Flavell, S. W. and Greenberg, M. E. (2008). Signaling mechanisms linking neuronal activity to gene expression and plasticity of the nervous system. *Annu. Rev. Neurosci.* **31**, 563-590.
Gamby, C., Waage, M. C., Allen, R. G. and Baizer, L. (1996). Analysis of the role of calmodulin binding and sequestration in neuromodulin (GAP-43) function. *J. Biol. Chem.* **271**, 26698-26705.
Ge, X., Qiu, Y., Loh, H. H. and Law, P. Y. (2009). GRIN1 regulates μ-opioid receptor activities by tethering the receptor and G protein in the lipid raft. *J. Biol. Chem.* **284**, 36521-36534.
Grabe, H. J., Schwahn, C., Mahler, J., Schulz, A., Spitzer, C., Fenske, K., Appel, K., Barnow, S., Nauck, M., Schomerus, G. et al. (2012a). Moderation of adult depression by the serotonin transporter promoter variant (5-HTTLPR), childhood abuse and adult traumatic events in a general population sample. *Am. J. Med. Genet. B. Neuropsychiatr. Genet.* **159B**, 298-309.
Grabe, H. J., Schwahn, C., Mahler, J., Appel, K., Schulz, A., Spitzer, C., Fenske, K., Barnow, S., Freyberger, H. J., Teumer, A. et al. (2012b). Genetic epistasis between the brain-derived neurotrophic factor Val66Met polymorphism and the 5-HTT promoter polymorphism moderates the susceptibility to depressive disorders after childhood abuse. *Prog. Neuropsychopharmacol. Biol. Psychiatry* **36**, 264-270.
Gutiérrez, G., Mendoza, C., Zapata, E., Montiel, A., Reyes, E., Montaño, L. F. and López-Marure, R. (2007). Dehydroepiandrosterone inhibits the TNF-alpha-induced inflammatory response in human umbilical vein endothelial cells. *Atherosclerosis* **190**, 90-99.
Hannan, M. A., Kabbani, N., Paspalas, C. D. and Levenson, R. (2008). Interaction with dopamine D2 receptor enhances expression of transient receptor potential channel 1 at the cell surface. *Biochim. Biophys. Acta* **1778**, 974-982.
Henley, J. R., Huang, K. H., Wang, D. and Poo, M. M. (2004). Calcium mediates bidirectional growth cone turning induced by myelin-associated glycoprotein. *Neuron* **44**, 909-916.
Hieber, V., Agranoff, B. W. and Goldman, D. (1992). Target-dependent regulation of retinal nicotinic acetylcholine receptor and tubulin RNAs during optic nerve regeneration in goldfish. *J. Neurochem.* **58**, 1009-1015.
Hilmas, C., Pereira, E. F., Alkondon, M., Rassoulpour, A., Schwarcz, R. and Albuquerque, E. X. (2001). The brain metabolite kynurenic acid inhibits α7 nicotinic receptor activity and increases non-α7 nicotinic receptor expression: physiopathological implications. *J. Neurosci.* **21**, 7463-7473.
Hruska, M. and Nishi, R. (2007). Cell-autonomous inhibition of α7-containing nicotinic acetylcholine receptors prevents death of parasympathetic neurons during development. *J. Neurosci.* **27**, 11501-11509.
Hu, M., Schurdak, M. E., Puttfarcken, P. S., El Kouhen, R., Gopalakrishnan, M. and Li, J. (2007). High content screen microscopy analysis of $A\beta_{1-42}$-induced neurite outgrowth reduction in rat primary cortical neurons: neuroprotective effects of α7 neuronal nicotinic acetylcholine receptor ligands. *Brain Res.* **1151**, 227-235.
Jian, X., Hidaka, H. and Schmidt, J. T. (1994). Kinase requirement for retinal growth cone motility. *J. Neurobiol.* **25**, 1310-1328.
Jouvenceau, A. and Dutar, P. (2006). A role for the protein phosphatase 2B in altered hippocampal synaptic plasticity in the aged rat. *J. Physiol. Paris* **99**, 154-161.
Kabbani, N. and Levenson, R. (2007). A proteomic approach to receptor signaling: molecular mechanisms and therapeutic implications derived from discovery of the dopamine D2 receptor signalplex. *Eur. J. Pharmacol.* **572**, 83-93.
Kabbani, N., Woll, M. P., Levenson, R., Lindstrom, J. M. and Changeux, J.-P. (2007). Intracellular complexes of the β2 subunit of the nicotinic acetylcholine receptor in brain identified by proteomics. *Proc. Natl. Acad. Sci. USA* **104**, 20570-20575.
Kaiser, P., Akerboom, T., Molnar, P. and Reinauer, H. (2008). Modified HPLC-electrospray ionization/mass spectrometry method for HbA_{1c} based on IFCC reference measurement procedure. *Clin. Chem.* **54**, 1018-1022.
Kano, Y., Hiragami, F., Kawamura, K., Kimata, Y., Nakagiri, S., Poffenberger, C. K., Akiyama, J., Okishima, K., Koike, Y. and Gomita, Y. (2002). Immunosuppressant FK506 induces sustained activation of MAP kinase and promotes neurite outgrowth in PC12 mutant cells incapable of differentiating. *Cell Struct. Funct.* **27**, 393-398.
Lauder, J. M. and Schambra, U. B. (1999). Morphogenetic roles of acetylcholine. *Environ. Health Perspect.* **107 Suppl. 1**, 65-69.
Lee, G., Newman, S. T., Gard, D. L., Band, H. and Panchamoorthy, G. (1998). Tau interacts with src-family non-receptor tyrosine kinases. *J. Cell Sci.* **111**, 3167-3177.
Leu, B., Koch, E. and Schmidt, J. T. (2010). GAP43 phosphorylation is critical for growth and branching of retinotectal arbors in zebrafish. *Dev. Neurobiol.* **70**, 897-911.
Lin, R., Karpa, K., Kabbani, N., Goldman-Rakic, P. and Levenson, R. (2001). Dopamine D2 and D3 receptors are linked to the actin cytoskeleton via interaction with filamin A. *Proc. Natl. Acad. Sci. USA* **98**, 5258-5263.
Lin, H., Vicini, S., Hsu, F. C., Doshi, S., Takano, H., Coulter, D. A. and Lynch, D. R. (2010). Axonal α7 nicotinic ACh receptors modulate presynaptic NMDA receptor expression and structural plasticity of glutamatergic presynaptic boutons. *Proc. Natl. Acad. Sci. USA* **107**, 16661-16666.
Lindstrom, J., Schoepfer, R., Conroy, W. G. and Whiting, P. (1990). Structural and functional heterogeneity of nicotinic receptors. *Ciba Found. Symp.* **152**, 23-42, discussion 43-52.
Liu, Q. and Berg, D. K. (1999). Actin filaments and the opposing actions of CaM kinase II and calcineurin in regulating α7-containing nicotinic receptors on chick ciliary ganglion neurons. *J. Neurosci.* **19**, 10280-10288.
Liu, Y. C. and Storm, D. R. (1989). Dephosphorylation of neuromodulin by calcineurin. *J. Biol. Chem.* **264**, 12800-12804.
Lopes, C., Pereira, E. F., Wu, H. Q., Purushottamachar, P., Njar, V., Schwarcz, R. and Albuquerque, E. X. (2007). Competitive antagonism between the nicotinic allosteric potentiating ligand galantamine and kynurenic acid at α7* nicotinic receptors. *J. Pharmacol. Exp. Ther.* **322**, 48-58.
Lowery, L. A. and Van Vactor, D. (2009). The trip of the tip: understanding the growth cone machinery. *Nat. Rev. Mol. Cell Biol.* **10**, 332-343.
Madsen, J. R., MacDonald, P., Irwin, N., Goldberg, D. E., Yao, G. L., Meiri, K. F., Rimm, I. J., Stieg, P. E. and Benowitz, L. I. (1998). Tacrolimus (FK506) increases neuronal expression of GAP-43 and improves functional recovery after spinal cord injury in rats. *Exp. Neurol.* **154**, 673-683.
Masuho, I., Mototani, Y., Sahara, Y., Asami, J., Nakamura, S., Kozasa, T. and Inoue, T. (2008). Dynamic expression patterns of G protein-regulated inducer of neurite outgrowth 1 (GRIN1) and its colocalization with Gαo implicate significant roles of Gαo-GRIN1 signaling in nervous system. *Dev. Dyn.* **237**, 2415-2429.
Mattson, M. P. (2008). Glutamate and neurotrophic factors in neuronal plasticity and disease. *Ann. N. Y. Acad. Sci.* **1144**, 97-112.
Mortimer, D., Fothergill, T., Pujic, Z., Richards, L. J. and Goodhill, G. J. (2008). Growth cone chemotaxis. *Trends Neurosci.* **31**, 90-98.
Myatt, D. R. and Nasuto, S. J. (2008). Improved automatic midline tracing of neurites with Neuromantic. *BMC Neurosci.* **9 Suppl. 1**, P81.
Nakata, H. and Kozasa, T. (2005). Functional characterization of Gαo signaling through G protein-regulated inducer of neurite outgrowth 1. *Mol. Pharmacol.* **67**, 695-702.
Owen, A. and Bird, M. (1995). Acetylcholine as a regulator of neurite outgrowth and motility in cultured embryonic mouse spinal cord. *Neuroreport* **6**, 2269-2272.
Pankratov, Y., Lalo, U., Krishtal, O. and Verkhratsky, A. (2002). Ionotropic P2X purinoreceptors mediate synaptic transmission in rat pyramidal neurones of layer II/III of somato-sensory cortex. *J. Physiol.* **542**, 529-536.
Paulo, J. A., Brucker, W. J. and Hawrot, E. (2009). Proteomic analysis of an α7 nicotinic acetylcholine receptor interactome. *J. Proteome Res.* **8**, 1849-1858.
Pereira, E. F., Hilmas, C., Santos, M. D., Alkondon, M., Maelicke, A. and Albuquerque, E. X. (2002). Unconventional ligands and modulators of nicotinic receptors. *J. Neurobiol.* **53**, 479-500.
Perry, D. C., Mao, D., Gold, A. B., McIntosh, J. M., Pezzullo, J. C. and Kellar, K. J. (2007). Chronic nicotine differentially regulates α6- and β3-containing nicotinic cholinergic receptors in rat brain. *J. Pharmacol. Exp. Ther.* **322**, 306-315.

Journal of Cell Science

Petros, T. J., Rebsam, A. and Mason, C. A. (2008). Retinal axon growth at the optic chiasm: to cross or not to cross. *Annu. Rev. Neurosci.* **31**, 295-315.
Rashid, T., Banerjee, M. and Nikolic, M. (2001). Phosphorylation of Pak1 by the p35/Cdk5 kinase affects neuronal morphology. *J. Biol. Chem.* **276**, 49043-49052.
Romano, S. J., Corriveau, R. A., Schwarz, R. I. and Berg, D. K. (1997). Expression of the nicotinic receptor α7 gene in tendon and periosteum during early development. *J. Neurochem.* **68**, 640-648.
Rüdiger, T. and Bolz, J. (2008). Acetylcholine influences growth cone motility and morphology of developing thalamic axons. *Cell Adh. Migr.* **2**, 30-37.
Sarma, T., Voyno-Yasenetskaya, T., Hope, T. J. and Rasenick, M. M. (2003). Heterotrimeric G-proteins associate with microtubules during differentiation in PC12 pheochromocytoma cells. *FASEB J.* **17**, 848-859.
Skene, J. H. (1989). Axonal growth-associated proteins. *Annu. Rev. Neurosci.* **12**, 127-156.
Skene, J. H. (1990). GAP-43 as a 'calmodulin sponge' and some implications for calcium signalling in axon terminals. *Neurosci. Res.* **13 Suppl,** S112-S125.
Slemmon, J. R., Morgan, J. I., Fullerton, S. M., Danho, W., Hilbush, B. S. and Wengenack, T. M. (1996). Camstatins are peptide antagonists of calmodulin based upon a conserved structural motif in PEP-19, neurogranin, and neuromodulin. *J. Biol. Chem.* **271**, 15911-15917.
Spitzer, N. C. (2012). Activity-dependent neurotransmitter respecification. *Nat. Rev. Neurosci.* **13**, 94-106.
Spitzer, T. L., Rojas, A., Zelenko, Z., Aghajanova, L., Erikson, D. W., Barragan, F., Meyer, M., Tamaresis, J. S., Hamilton, A. E., Irwin, J. C. et al. (2012). Perivascular human endometrial mesenchymal stem cells express pathways relevant to self-renewal, lineage specification, and functional phenotype. *Biol. Reprod.* **86**, 58.
Stefan, M. I., Edelstein, S. J. and Le Novère, N. (2008). An allosteric model of calmodulin explains differential activation of PP2B and CaMKII. *Proc. Natl. Acad. Sci. USA* **105**, 10768-10773.
Stiess, M. and Bradke, F. (2011). Neuronal polarization: the cytoskeleton leads the way. *Dev. Neurobiol.* **71**, 430-444.
Stone, T. W. and Darlington, L. G. (2002). Endogenous kynurenines as targets for drug discovery and development. *Nat. Rev. Drug Discov.* **1**, 609-620.
Strittmatter, S. M., Valenzuela, D., Vartanian, T., Sudo, Y., Zuber, M. X. and Fishman, M. C. (1991). Growth cone transduction: Go and GAP-43. *J. Cell Sci.* **15** Suppl, 27-33.
Strittmatter, S. M., Fishman, M. C. and Zhu, X. P. (1994a). Activated mutants of the α subunit of G_o promote an increased number of neurites per cell. *J. Neurosci.* **14**, 2327-2338.
Strittmatter, S. M., Igarashi, M. and Fishman, M. C. (1994b). GAP-43 amino terminal peptides modulate growth cone morphology and neurite outgrowth. *J. Neurosci.* **14**, 5503-5513.
Swarzenski, B. C., O'Malley, K. L. and Todd, R. D. (1996). PTX-sensitive regulation of neurite outgrowth by the dopamine D3 receptor. *Neuroreport* **7**, 573-576.
Takemura, M., Mishima, T., Wang, Y., Kasahara, J., Fukunaga, K., Ohashi, K. and Mizuno, K. (2009). Ca^{2+}/calmodulin-dependent protein kinase IV-mediated LIM kinase activation is critical for calcium signal-induced neurite outgrowth. *J. Biol. Chem.* **284**, 28554-28562.
Vallejo, Y. F., Buisson, B., Bertrand, D. and Green, W. N. (2005). Chronic nicotine exposure upregulates nicotinic receptors by a novel mechanism. *J. Neurosci.* **25**, 5563-5572.
van Kesteren, R. E. and Spencer, G. E. (2003). The role of neurotransmitters in neurite outgrowth and synapse formation. *Rev. Neurosci.* **14**, 217-231.
Wen, Z., Guirland, C., Ming, G. L. and Zheng, J. Q. (2004). A CaMKII/calcineurin switch controls the direction of Ca^{2+}-dependent growth cone guidance. *Neuron* **43**, 835-846.
Yamatani, H., Kawasaki, T., Mita, S., Inagaki, N. and Hirata, T. (2010). Proteomics analysis of the temporal changes in axonal proteins during maturation. *Dev. Neurobiol.* **70**, 523-537.
Yang, H., Wan, L., Song, F., Wang, M. and Huang, Y. (2009). Palmitoylation modification of $G\alpha_o$ depresses its susceptibility to GAP-43 activation. *Int. J. Biochem. Cell Biol.* **41**, 1495-1501.
Zheng, J. Q., Felder, M., Connor, J. A. and Poo, M. M. (1994). Turning of nerve growth cones induced by neurotransmitters. *Nature* **368**, 140-144.
Zhou, F. Q., Waterman-Storer, C. M. and Cohan, C. S. (2002). Focal loss of actin bundles causes microtubule redistribution and growth cone turning. *J. Cell Biol.* **157**, 839-849.

Journal of Cell Science

Table S1. Intracellular proteins that co-immunoprecipitate with α7 from differentiating PC12 cells.

nAChRs:	Protein Score	MW (Da)	NCBI	Number of Peptides
α7	8.08	56373.4	71896614	4
G Protein Complex:				
Gprin1	46.08	85066.5	62663260	8
$G\alpha_i$	2.05	44988.0	62647168	2
$G\alpha_o$	10.10	40042.9	8394152	2
GAP-43	8.05	23589.3	8393415	4
Kinases & Phosphatases:				
Calcineurin (PP2B)	10.06	58372.0	62666988	5
CaMKIIβ	6.04	30834.4	62658192	3
PKCβ	6.06	44231.0	62656037	1
PKCδ	6.06	58763.5	34852266	1
PKCη	6.08	22309.6	62656086	3
Calmodulin 3	28.06	63326.3	62639070	5
Cytoskeletal Regulators:				
Arp2/3	20.07	203429.1	62665219	2
Cdc42	8.05	21245.0	61889112	1
Cofilin	18.07	10747.7	62718769	3
PAK 1	30.07	68501.4	56799432	4
p32a	20.09	38453.3	21617859	2
p32b	8.03	54850.6	21955259	1

Cytoskeletal Components:				
α Tubulin	4.05	49990.0	62663792	5
β Actin	20.06	46840.3	62663393	3
α7 nAChR Regulators:				
Ric-8a	14.11	52594.4	57528201	2
Src-Family Phosphoprotein 1	4.07	106424.9	62652127	1
Src-Family Phosphoprotein 2	4.07	37463.8	17105340	1
Vesicle Trafficking:				
Synapsin 1	8.06	52421.5	9507161	5
Synapsin 2	42.08	73942.7	9507159	2
Synapsin 3	28.07	63308.9	8394389	6
Synaptotagmin 9	40.09	47179.2	6981624	9
Synaptophysin	8.06	33289.1	6981622	1

Table S2. In-gel digest of intracellular proteins which co-immunoprecipitate with the α7 subunit in differentiating PC12 cells.

MW (kDa)	Band Identity	Peptides	Protein Score	NCBI
85	Gprin1	KAPSWDAGAPPPRE	20.07	62663260
62	GAP-43	KEGDGSATTDAAPATSPKA	12.06	8393415
62	Calmodulin 3	RHVMTRLGEKL	8.06	62639070
55	α7	RPACQHKPRRC	18.06	71896614
43	GAP-43	RTKQVEKNDEDQK	8.04	8393415
42	$G\alpha_o$	KQMKIIHEDGFSGEDVKQYKP	8.07	8394152
20	Calmodulin 3	RVFDKDGNGYISAAELRH	8.06	62639070

Table S3. In-gel digest of crosslinked intracellular proteins that stain for GAP-43.

MW (kDa)	Band Identity	Peptides	Protein Score	NCBI
62	GAP-43	RGHITRK	9.03	8393415
62	Calmodulin 3	KDGNGYISAAELRH	8.03	62639070
43	GAP-43	KQVEKNDEDQKI	6.05	8393415

Table S4. In-gel digest of intracellular proteins which co-immunoprecipitate with Gprin1 in differentiating PC12 cells.

MW (kDa)	Band Identity	Peptides	Protein Score	NCBI
85	Gprin1	RAPEKGNPGNSTRV	20.07	62663260
62	GAP-43	KEDPEADQEHA	12.06	8393415
62	Calmodulin 3	READIDGDGQVNYEEFVQMMTA	8.06	62639070
55	α7	MCGGRG	18.06	71896614
43	GAP-43	KGDAPAAEAEAKEKD	8.04	8393415
42	$G\alpha_o$	KMVCDVVSRM	6.03	8394152
20	Calmodulin 3	RKMKDTDSEEEIRE	8.07	62639070